Asian Journal of Chemistry; Vol. 33, No. 12 (2021), 3056-3062

ASIAN JOURNAL OF CHEMISTRY

https://doi.org/10.14233/ajchem.2021.23480

Quantum Chemical Computational Studies on *N*-Acetylglycine Single Crystal for Potential Applications

R. USHA[1], N. KANAGATHARA[1,*] and V.J. THANIGAIARASU[2]

[1]Department of Physics, Saveetha School of Engineering, Saveetha Institute of Medical and Technical Sciences, Thandalam, Chennai-602105, India
[2]Department of Physics, Jaya College of Arts and Science, Thiruninravur, Chennai-602024, India

*Corresponding author: E-mail: kanagathara23275@gmail.com

Received: 16 August 2021; *Accepted*: 25 September 2021; *Published online*: 6 December 2021; AJC-20598

The crystals of *N*-acetylglycine were obtained by the slow evaporation of an aqueous solution at room temperature. Single crystal X-ray diffraction analysis reveals that the crystal belongs to monoclinic system with centro symmetric space group $P2_1/c$ with lattice parameters are a = 4.8410(10) Å, b = 11.512(2) Å, c = 9.810(2) Å, α = 90º, β = 97.02(3)º, γ = 90º and V = 542.61 (Å)^3. Quantum chemical computations have been performed on the grown crystal with DFT-B3LYP/6-311++G(d,p) basis set. The theoretically obtained geometrical parameters and vibrational frequencies are in close agreement with experimental data. HOMO-LUMO energy gap and molecular electrostatic potential map has also been calculated. The static and dynamic polarizability and first hyperpolarizability both were calculated to comprehend the potential applications of *N*-acetylglycine in nonlinear optics. Hirshfeld surface analysis has been performed to study the inter and intra molecular interactions between the molecule. Thus in present study, the structure-property relationship of novel *N*-acetylglycine molecule is studied for future nonlinear optical applications through experimental and theoretical approach.

Keywords: N-acetylglycine, B3LYP/6-311++G(d,p), NBO, NLO, Hirshfeld surface analysis.

INTRODUCTION

True computational prediction of material properties before experimentation is needed for finding the new materials for its application. Theoretical computational studies enable us to go well beyond what is known experimentally and it can guide future experimentation. Accurate quantum treatment of chemical effects can predict geometries, vibrational frequencies, NMR chemical shifts, relative stabilities of families of isomers, activation energies and reaction energies for organic, inorganic and organometallic systems. The knowledge of molecular equilibrium geometries helps to understand the electronic structure, thermodynamic stability and chemical reactivity of molecules. Quantum mechanical chemistry plays a vital role in the prediction of materials development by simulation techniques like density functional theory. This theoretical techniques lead to dramatic advances in the science of materials. Density functional theory is the prominent method of computing molecular structure, vibrational frequencies and energies of molecules and yield potential structural and conformational information about the molecule. *N*-Acetylglycine is popular for its applications in drug research and is the building block for few amino acids. There are many reports available about the physical, chemical as well as other properties of *N*-acetylglycine [1-5]. Thanigaiarasu *et al.* [6,7] reported the structural, optical, photoluminescence, thermal and mechanical properties of *N*-acetylglycine. In continuation of studies on *N*-acetylgycine, the present study is aimed to perform all the above mentioned calculations by using Gaussian 09 program with 6-311++G (d,p) basis set and were analyzed with the help of Gauss View program. The vibrational assignments of the normal modes can be provided based on the potential energy distribution which was accomplished with VEDA program. Also the efforts will be made to get hyperpolarizability calculations to know the nonlinear optical behaviour of the compound.

EXPERIMENTAL

The obtained *N*-acetylglycine crystals is then subjected to single crystal XRD by using KUMA 4-diffractometer [6,7].

In present investigation, DFT calculations were performed with a hybrid functional B3LYP at 6-311++G(d,p) basis set using Gaussian 09 program [8]. Structure is optimized with minimum energy. The harmonic frequencies, infrared and Raman intensities were calculated by the B3LYP method with an identical basis set. All the frequencies are scaled by 0.9665. The absence of imaginary values of wavenumbers on the calculated vibrational spectra confirms that the deduced structure corresponds to the minimum energy. The NBO and HOMO-LUMO orbital energies were investigated and the visual inter-pretation of the above mentioned properties were done by using Gauss View 3.1 program [9,10].

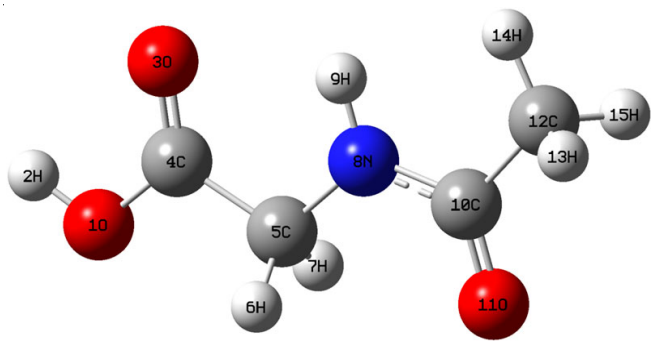

Fig. 1. Optimized structure of *N*-acetylglycine

RESULTS AND DISCUSSION

Structural description: Single crystal X-ray diffraction analysis reveals that the crystal belongs to monoclinic system with centro symmetric space group $P2_1/c$ with lattice parameters are a = 4.8410(10) Å, b = 11.512(2) Å, c = 9.810(2) Å, α = 90º, β = 97.02(3)º, γ = 90º and V = 542.61 (Å)^3 [6]. Table-1 listed the bond distances and bond angles of experimental [6] and computed data obtained from the DFT calculation using the method B3LYP with the basis set 6-311++G(d,p). Structure is optimized with global minimum. Fig. 1 depicts the optimized structure of *N*-acetylglycine. C-H bond distance is about 0.970 Å and this value is computed to be 1.095 Å. C-N bond distance is 1.438 Å and computational value is 1.444 Å. However, the N1-C3 is found to be 1.329 Å and computational value is 1.364 Å. C1-C2 and C3-C4 bond distance is calculated to be 1.503 and 1.483 Å. Theoretical values of those bond values are found to be 1.509 and 1.516 Å, respectively. Similarly bond angles of C-O-H, O-C-O, N-C-C, C-C-H, O-C-N, H-C-H values are listed in Table-1. It is observed that all the bond distances and bond angles obtained experimentally is coincide with the theoretical values. However, the variation in theoretical values is due to the calculation is done in gas phase.

Vibrational spectrum: Quantum mechanical calculation of vibrational spectra can facilitate the interpretation of the observed spectra. Performing DFT calculations to provide deep insight into the vibrational spectrum and molecular parameters. A reliable assignment of the experimentally observed IR and Raman bands provides a clear understanding of the geometry and structure of the molecule. Theoretical simulations can assist in obtaining a deeper understanding of the vibrational spectra of complicated molecules. The DFT method is an efficient tool for the comparison between the vibrational spectra and quantum chemical calculations. Theoretical prediction of vibrational frequencies are listed in Table-2. Figs. 2 and 3 presented the theoretically predicted and experimental FT-IR and FT Raman spectrum. There are 15 elements (*m.f.* $C_4H_7NO_3$) in *N*-acetylglycine and the number of vibrational degrees of freedom of this nonlinear molecule 39 based on 3n-6. Vibrations includes 14 stretching, 13 bending and 12 torsional vibrations. The strong infrared peak at 3355 cm^{-1} is attributed to the asymmetric stretching vibration N-H and this peak is theoretically computed at 3492 cm^{-1}. Similarly, C-H asymmetric and symmetric stretching vibrations occur 3085, 2925 and 2852 cm^{-1} with weak intensity are computed at 3015, 3013 and 2955 cm^{-1}. Carboxyl group vibrations occur at 1722 cm^{-1} in infrared spectrum with medium intensity and 1710 cm^{-1} with weak intensity. This peak is computed at 1750 and 1441 cm^{-1}. The C-N and C-C stretching vibrations are computed at 1432 and 1423, 1367 cm^{-1}. The medium infrared and Raman peak at 1379 and 1377 cm^{-1} is ascribed to C-O-H bending vibration. This peak is theoretically computed at 1351 cm^{-1}. C-N-H bending vibration is

TABLE-1
OBSERVED AND COMPUTED BOND DISTANCES (Å) AND BOND ANGLES (°)

Bond distance (Å)			Bond angle (°)			Bond angle (°)		
Atom	Expt. [Ref. 6]	DFT B3LYP/6-311++G(d,p)	Atom	Expt. [Ref. 6]	DFT B3LYP/6-311++G(d,p)	Atom	Expt. [Ref. 6]	DFT B3LYP/6-311++G(d,p)
O1-C1	1.304	1.347	C1-O1-H1	110.0	107.694	C3-C4-H42	109.5	108.613
O1-H1	0.900	0.969	O2-C1-O1	125.1	123.460	H41-C4-H42	109.5	109.164
O2-C1	1.197	1.206	O2-C1-C2	123.4	125.192	C3-C4-H43	109.5	113.605
C1-C2	1.503	1.509	O1-C1-C2	111.5	123.460	H41-C4-H43	109.5	109.161
C2-N1	1.438	1.444	N1-C2-C1	110.8	109.743	H42-C4-H43	109.5	107.504
C2-H21	0.970	1.095	N1-C2-H21	109.5	111.564	O3-C3-C4	122.3	122.421
C2-H22	0.970	1.095	C1-C2-H21	109.5	108.969	N1-C3-C4	117.6	115.825
N1-C3	1.329	1.364	N1-C2-H22	109.5	111.548	C3-C4-H41	109.5	108.615
N1-H2	0.850	1.009	C1-C2-H22	109.5	108.976	C3-N1-H2	117.1	121.731
C3-O3	1.232	1.221	H21-C2-H22	108.1	105.926	C2-N1-H2	122.1	121.752
C3-C4	1.483	1.516	C3-N1-C2	120.6	121.254	O3-C3-N1	120.1	117.013
C4-H41	0.960	1.091						
C4-H42	0.960	1.091						
C4-H43	0.960	1.091						

TABLE-2
EXPERIMENTAL AND THEORETICALLY COMPUTED FT-IR AND FT RAMAN DATA OF *N*-ACETYLGLYCINE

Unscaled frequency (cm^{-1})	Scaled frequency (cm^{-1})	Experiment [Ref. 6]		DFT/B3LYP/6-311++G(d,p)		Band assignment description
		IR	Raman	IRs Intensity (arb. unit)	Raman activity (arb. unit)	
3759	3633			88.885	129.44	1O-2H stretching
3613	3492	3355 vs		72.182	56.569	8N-9H stretching
3120	3015	3085w		16.432	55.414	5C-6H stretching
3117	3013	2925 m	2937 m	4.9104	68.118	5C-7H stretching
3058	2955	2852 m		3.4002	53.653	12C-13H stretching
3045	2943			7.747	161	12C-14H stretching
3037	2935			20.192	121.51	12C-15H stretching
1811	1750	1722 m	1710 w	258.13	11.676	3O-4C stretching
1737	1679	1583 s		371.71	8.4979	11O-10C stretching
1534	1482			260.26	2.17	8N-10C stretching
1491	1441			33.52	2.9539	1O-4C stretching
1482	1432			6.3015	7.6063	8N-5C stretching
1472	1423			7.5891	6.5631	4C-5C stretching
1415	1367			232.18	0.9464	12C-10C stretching
1398	1351	1379 m	1377 w	1.3667	1.4534	2H-1O-4C bending
1312	1268	1350 m		0.1114	6.3428	9H-8N-5C bending
1257	1215	1277 m		12.952	8.7363	6H-5C-4C bending
1239	1198	1226 w	1228 w	0.3546	5.9013	7H-5C-6H bending
1182	1143			178.9	3.4666	13H-12C-15H bending
1142	1104			151.68	0.0775	14H-12C-13H bending
1057	1021	1146 m	1136 m	6.502	0.0568	15H-12C-14H bending
1013	979.4	1051 m		3.1746	0.3191	3O-4C-1O bending
1005	970.9			16.223	7.427	11O-10C-12C bending
986.9	953.8	992 m	1002 s	24.292	6.8594	1O-4C-5C bending
872.6	843.3	905 m	895 vw	4.5759	1.5018	5C-8N-10C bending
648	626.3	840 w		105.29	0.0621	4C-5C-8N bending
642	620.4	716 w		13.405	10.08	12C-10C-8N bending
638.3	616.9	600 w	590 w	10.466	1.0458	2H-1O-4C-5C bending
617.8	597.1			14.437	0.5671	9H-8N-10C-12C bending
514.4	497.1	548 w	555 w	5.2154	2.7045	6H-5C-4C-1O bending
501.5	484.7			48.683	0.3061	7H-5C-4C-1O bending
473.6	457.8			85.149	0.1772	13H-12C-10C-8N bending
350.2	338.5	410 w	397 w	0.4421	1.5405	14H-1O-10C-8C bending
270	260.9			0.1901	1.3468	15H-12C-10C-8N bending
181.8	175.7			13.853	0.5502	1O-4C-5C-8N bending
131.2	126.8			12.752	0.0677	4C-5C-8N-10C bending
71.98	69.57			0.9894	0.1493	12C-10C-8N-5C bending
58.25	56.3			4.3956	0.1393	3O-5C-1O-4C bending
33.08	31.98			2.7343	0.3783	11O-12C-8N-10C bending

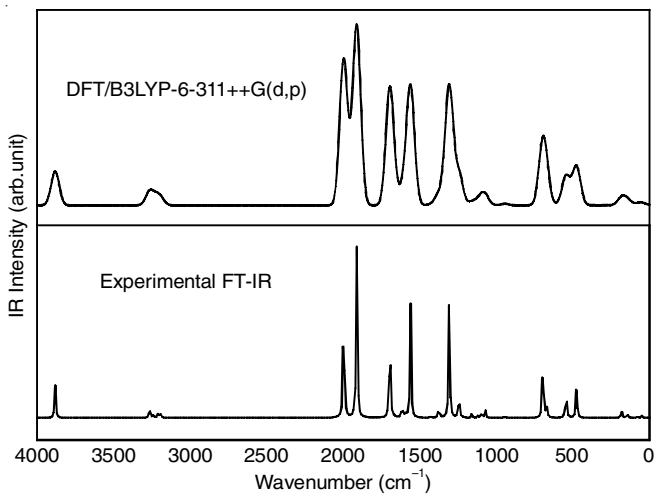

Fig. 2. Theoretical & experimental FT-IR spectrum of *N*-acetylglycine

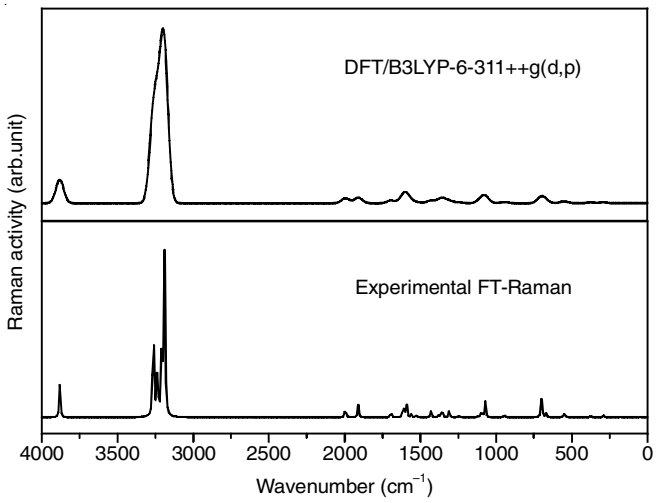

Fig. 3. Theoretical & experimental FT-Raman spectrum of *N*-acetylglycine

computed at 1268 cm^{-1}. The bending vibration H-C-H atoms are computed at 1215, 1198, 1143, 1104 and 1021 cm^{-1} and experimentally observed 1277, 1226 and 1146 cm^{-1} with weak intensity in infrared spectrum. The corresponding Raman peaks observed at 1228 and 1136 cm^{-1}. The other bending and torsional vibrations are listed in Table-2 with assignment description. All the theoretical values are coincide with experimental values [6].

Natural Bonding orbital analysis: Fig. 4 shows the NBO charges computed for the given molecule. According to the computation, the carbon atoms attached to oxygen atom have positive charge 0.21e. Oxygen and nitrogen atoms attached hydrogen have a positive charge 0.292e and 0.277e, respectively. Methyl group hydrogen atoms vary from 0.12 to 0.18e. Carboxyl group attached carbon atoms has positive charge 0.210e whereas the methyl group attached carbon has negative charge -569e. Also carbon atom of CH_2 group has a negative charge of -0.357e. The negative charges are balanced by the positive charges on the hydrogen atoms. Thus natural bonding orbital analysis gives the distribution of charges in the atoms and explain the stability of the atom. Also NBO analysis is used to study an inter and intramolecular interactions among the molecules [11,12]. The selected donor-acceptor interactions based on second order perturbation Fock-matrix theory is listed in Table-3. The delocalization of electron from filled Lewis type NBO to non-Lewis type NBO results in hyperconjugation effect. For each donor (i) and acceptor (j), the stabilization energy E(2)

$$E(2) = \Delta E_{ij} = q_i \quad (1)$$

where q_i is the occupancy of donor orbital, E_i and E_j are energies of donor and acceptor orbital's and F(i,j) is the NBO Fock matrix element [13-15]. The computed NBO analysis based on second-order perturbation theory at B3LYP/6-31G(d.p) level is listed in Table-3. As the chosen molecule is single one, it is expected that only intramolecular stabilization energy.

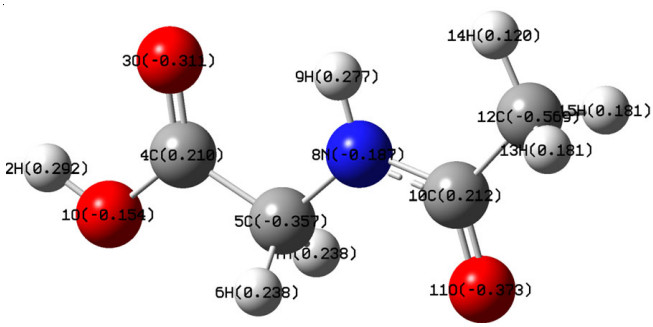

Fig. 4. NBO charges of *N*-acetylglycine

TABLE-3
SECOND-ORDER PERTURBATION THEORY ANALYSIS OF THE FOCK MATRIX IN NBO BASIS CALCULATED AT B3LYP/6-31G(d.p) LEVEL

Donor (i)	Acceptor (j)	$E^{(2)}$ (Kj mol^{-1})	E(j)-E(i) (a.u)	F(i.j) (a.u)
LP (2) O1	BD*(2) O3-C4	51.64	0.36	0.123
LP (2) O3	BD*(1) O1-C 4	31.59	0.68	0.133
LP (2) O3	BD*(1) C4-C5	19.57	0.66	0.103
LP (1) N8	BD*(2) C10-O11	64.65	0.30	0.125
LP (2) O11	BD*(1)N 8-C 10	22.08	0.76	0.117
LP (2) O11	BD*(1) C10-C12	17.91	0.66	0.099

Highest value of 64.65 kJ mol^{-1} is found between lone pair of nitrogen atom (N8) and π*(C10-O11) and the next highest intramolecular stabilization is 51.64 kJ mol^{-1} that occurs in between lone pair of oxygen O1 atoms with π*(O3-C4). The lone pair of oxygen atom (O3) with σ*(O1-C4) & σ*(C4-C5) has a stabilization energy value of 31.59 and 19.57 kJ mol^{-1}, respectively. Oxygen atom (O11) has an intramolecular stabilization energy of 22.08 and 17.91 kJ mol^{-1} with respect the σ*(N8-C10) and σ*(C10-C12) transition.

Frontier molecular orbital analysis: Frontier molecular orbital computational method generally viewed as a nucleophilic (HOMO) and electrophilic (LUMO) nature of the molecular system. Fukui developed the frontier molecular orbital theory to explain the HOMO-LUMO interactions of the molecule and describe the chemical reactivity of the sample [16]. Fig. 5 represents the HOMO-LUMO plot of *N*-acetylglycine. Lone pair of electrons present in the LUMO orbital as nitrogen is more electronegative than carbon. Electronegativity of oxygen is lower than nitrogen hence LUMO is completely occupied in the *N*-acetylglycine molecule and possess lesser energy value of -3.798 eV. HOMO is occupied completely surrounding nitrogen *i.e.* CH_2, C-O, N-H and possess the high value of -10.020 eV. The high value of HOMO indicates the good nucleophilic due to carbonyl group and the lower value of LUMO indicates the good electrophilic nature of the grown crystal. From the structure, it is predicted that nitrogen reacts with carbonyl intramolecularly and become close to carbonyl group. This lengthen the C-O bond and make the carbonyl carbon becomes pyramidalized. The energy gap between HOMO-LUMO is 6.222 eV, which represents that the molecule is highly stable and less chemically active. Thus, the HOMO-LUMO analysis confirms the presence of charge transfer that occurs within the molecule and support the bioactivity of the grown crystal. By taking into consideration the values of HOMO and LUMO other electronic parameters like global hardness, chemical potential, electrophilicity can be calculated [17-19] and are listed in Table-4.

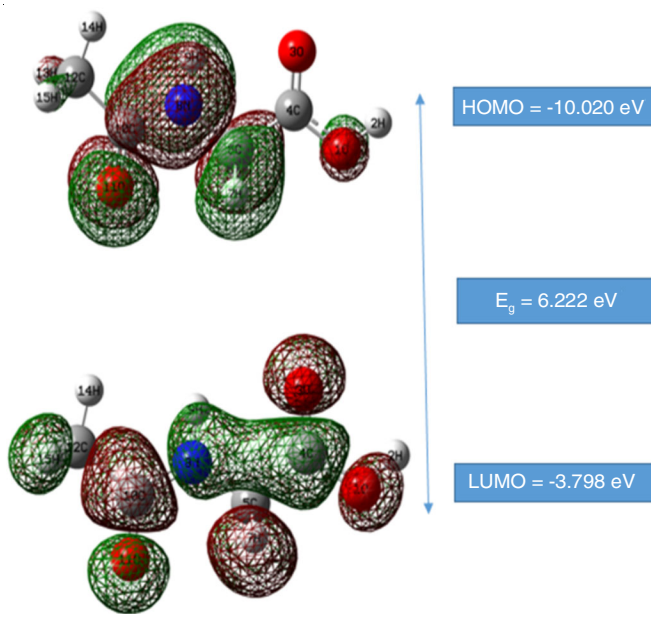

Fig. 5. HOMO-LUMO plot of *N*-acetylglycine

TABLE-4
HOMO-LUMO ENERGY VALUE AND RELATED PROPERTIES OF *N*-ACETYLGYCINE CALCULATED BY B3LYP/6-311++G(d,p) METHOD

E_{HOMO} (eV)	-10.020
E_{LUMO} (eV)	-3.798
Energy gap ΔE (eV)	6.222
Ionization potential (A) (eV)	+10.020
Electron affinity (I)	+3.798
Global softness (S)	0.160
Global hardness (η)	3.111
Chemical potential (?)	6.909
Global electrophilicity (ω)	6.763

Molecular electrostatic potential (MEP) analysis: The mole-cular electrostatic potential, v(r), at a given point r (x, y, z) in the vicinity of a molecule, is expressed in terms of the interaction energy between the electrical charge originated from the mole-cule electrons, nuclei and a positive test charge (Z_A a proton) located at r. Molecular electrostatic potential map is given by the equation [20-22]:

$$V(r) = \sum_{A}^{Na} \frac{Z_A}{|r - R_A|} - \int \frac{\rho(r')d^3r'}{|r - r'|} \quad (2)$$

The first term is the bare nuclear potential and the second term is the electronic contribution. This is related to the electronic density and is a useful descriptor for determining sites for electro-philic attack and nucleophilic reactions as well as hydrogen-bonding interactions which is represented by a colour grading. Fig. 6 represents the molecular electrostatic potential map of *N*-acetylglycine. Electrostatic potential ranges from -3.106 × 10^{-2} to +3.106 × 10^{-2}. Electophilic and nucleophilic reactivity is represented by the red and blue colour, respectively and green colour for the zero potential. Fig. 6 showed that the oxygen atoms has negative electropotential indicated by red colour and the hydrogen atoms are indicated blue colour and has the positive charge. These sites explore the existence of non-covalent interactions in the molecule.

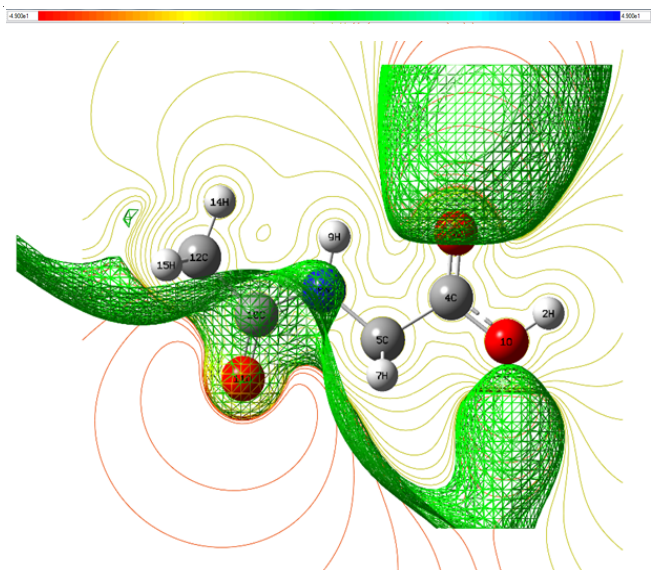

Fig. 6. Molecular electrostatic potential map

First order hyperpolarizability computations: Gaussian 09W program using B3YLP/6-311++G(d,p) methodology is applied to get the total molecular dipole moment (m), linear polarizability (α) and first-order hyperpolarizability (b). The computed results in atomic units and are converted into electro-static units (α: 1a.u = 0.1482 × 10^{-24} esu, β: 1a.u = 8.6393 × 10^{-30} esu). Table-5 summarize the calculated parameters of an electric dipole moment μ(D), the average polarizability α_{tot} (× 10^{-24} esu) and first order hyperpolarizability b_{tot} (× 10^{-31} esu). The calculated dipole moment is 2.7111 Debye and it is high in the Y as well as Z directions. The first order hyperpolarizability value (b_{tot}) is found to be 60.7974 ×$10^{"31}$ esu which is compared with urea (3.7289 × 10^{-31} esu) and shows that the grown crystal is 16.045 times that of urea. Hence, it is expected this material may be suitable candidate for nonlinear optical applications [23-25].

TABLE-5
ELECTRIC DIPOLE MOMENT μ(D). THE AVERAGE POLARIZABILITY α_{tot} (× 10^{-24} esu) AND FIRST HYPERPOLARIZABILITY β_{tot} (× 10^{-31} esu)

Parameters	B3LYP/6-311G(d,p)	Parameters	B3LYP/6-311G(d,p)
μ_x	-1.9498	β_{xxx}	-51.9982
μ_y	1.8837	β_{xxy}	17.5532
μ_z	0.0028	β_{xyy}	-1.9794
μ(D)	2.7111	β_{yyy}	3.4807
α_{xx}	-42.1535	β_{zxx}	-0.0109
α_{xy}	9.5100	β_{xyz}	-0.0145
α_{yy}	-54.6237	β_{zyy}	0.0133
α_{xz}	0.0063	β_{xzz}	-3.0605
α_{yz}	-0.0019	β_{yzz}	-1.7669
α_{zz}	-46.4100	β_{zzz}	-3.0605
α_{tot} (e.s.u)	47.7291 × 10^{-24}	β_{tot} (e.s.u)	60.7974 × 10^{-31}

Hirshfeld surface analysis: Hirshfeld surface analysis of *N*-acetylglycine was performed with the Crystal Explorer 3.1 program [26] using the experimental structure as input to reveal intermolecular interactions in the crystal. Fig. 7 represents 100% fingerprint of *N*-acetylglycine. The results presented in Figs. 8 and 9, shows the 3D Hirshfeld surface (d_{norm}) and 2D fingerprint histogram of the molecule respectively. In Fig. 2, the red coloured points represent the intermolecular contacts shorter than the sum of their van der Waals radii (hydrogen bonds) while contacts greater than this sum are blue colour and white colours represent contacts around the sum of the van der Waals radii [27]. The d_{norm} values were determined to be in the range -0.1192 (negative points-red) to 1.2894 (positive points-blue) Å. In Fig. 2, C-H···O and C-H···N contacts are marked with green dashed lines with the C-H···O hydrogen bonds having a length of 2.443 Å and 2.916 Å, while the C-H···N hydrogen bonds have a length of 2.819 Å and 2.639 Å.The 2D fingerprint histograms shown in Fig. 3 indicate the contributions of the intermolecular contacts to the Hirshfeld surfaces to be H···H (40.5%), N···H/H···N (1.4%), O···H/H···O (48.6%) and C···H/H···C (2.0%), respectively with included reciprocal interactions.

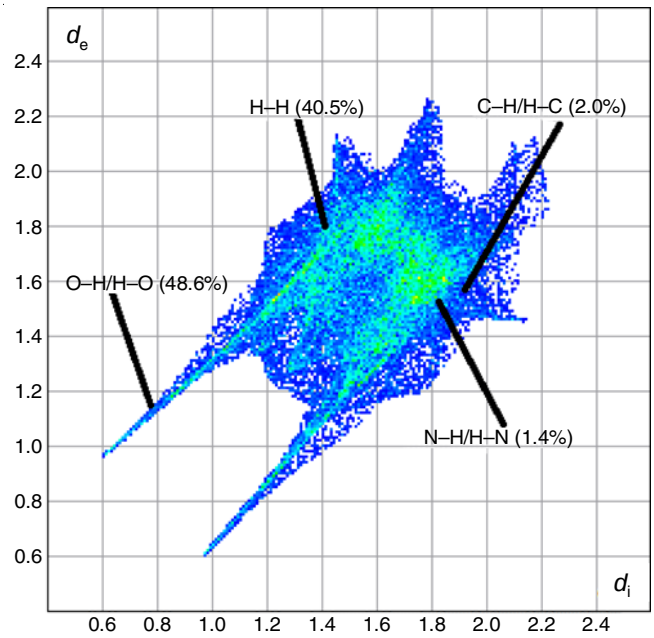

Fig. 7. Fingerprint of *N*-acetylglycine (100%)

Conclusion

Present study is aimed to know the structure-property relationship of *N*-acetylglycine molecule for future nonlinear optical applications through experimental and theoretical approach. Theoretical quantum chemical computations have been performed on the *N*-acetylglycine with DFT-B3LYP/6-311++G(d,p) basis set. The obtained structural and vibrational parameters are very well coincide with the experimental values. Frontier molecular orbital analysis explain the charge transfer among the molecule and describes the HOMO-LUMO interactions as well as chemical reactivity of the obtained compound. The existence of intramolecular stabilization within the molecule is described by natural bonding orbital analysis. Molecular electrostatic potential map explores the molecular bonding as well as chemical reactivity of the grown crystal. 3D Hirshfeld surface (d_{norm}) and 2D fingerprint plot of *N*-acetylglycine gives the visual representation of intermolecular contact within the material. The total dipole moment is calculated to be 2.711 Debye. First order hyperpolarizability calculations reveals that *N*-acetylglycine 16.045 times that of urea. Hence, it is expected that the grown material may be suitable candidate for nonlinear optical applications.

CONFLICT OF INTEREST

The authors declare that there is no conflict of interests regarding the publication of this article.

REFERENCES

1. S. Bee, N. Choudhary, A. Gupta and P. Tandon, *Biopolymers*, **101**, 795 (2014); https://doi.org/10.1002/bip.22458

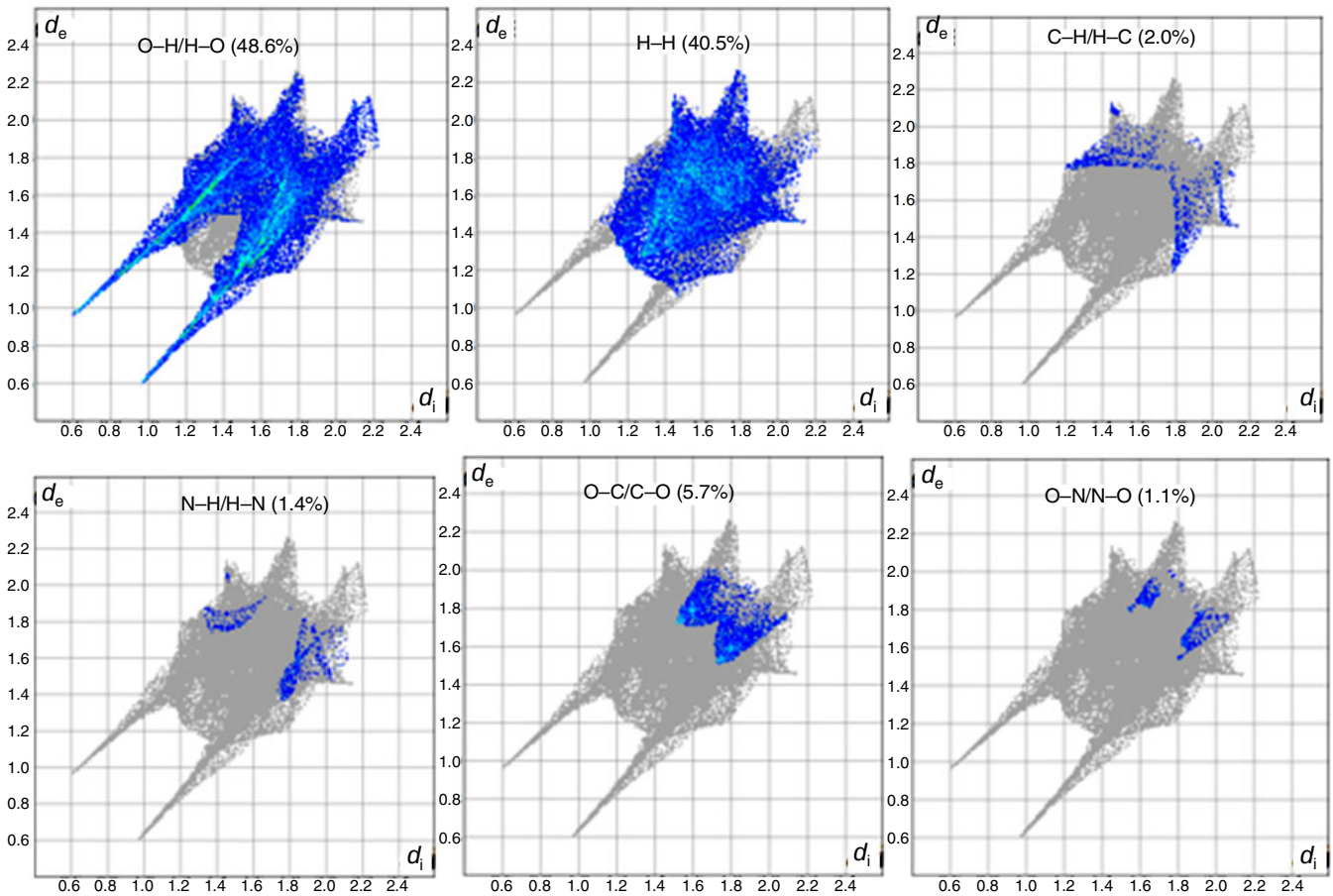

Fig. 8. Relative contributions to the percentage of Hirshfeld surface area for the various intermolecular contacts in *N*-acetylglycine

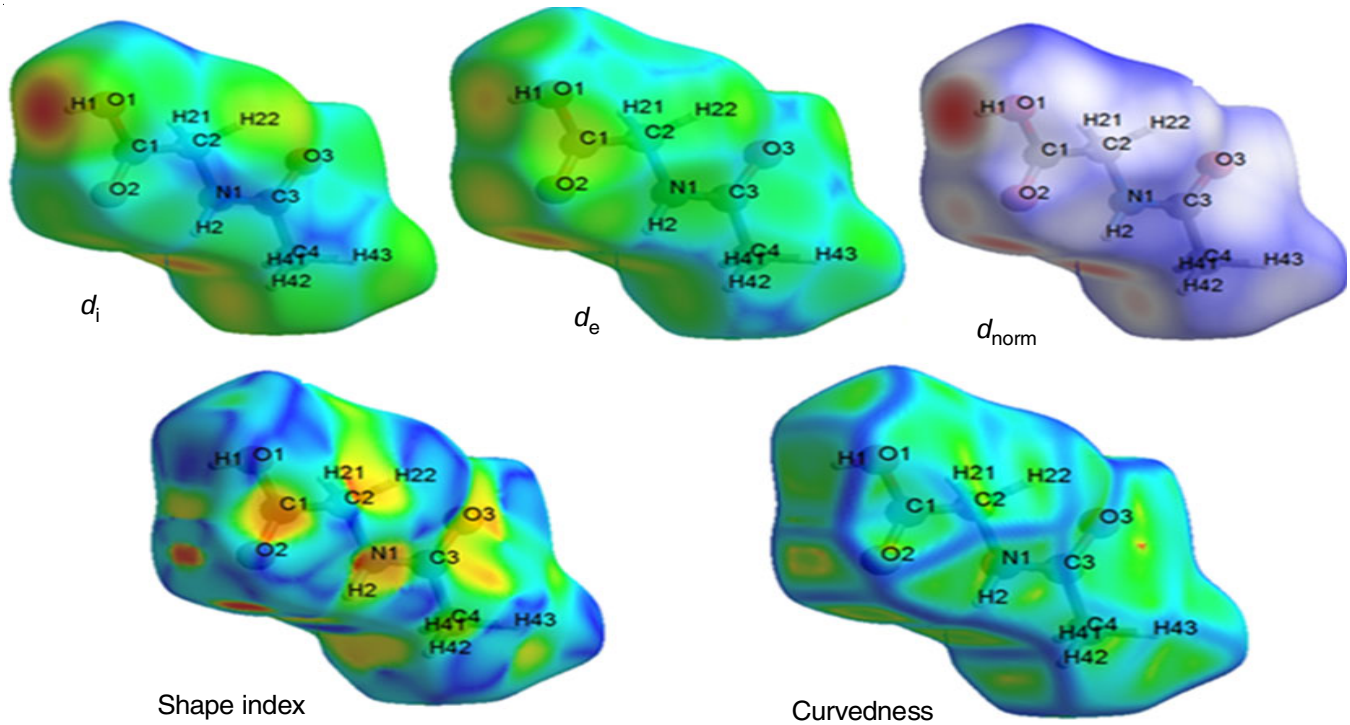

Fig. 9. Hirshfeld surface analysis d_i, d_e, d_{norm}, shape index and curvedness of *N*-acetylglycine

2. B. Boeckx and G. Maes, *J. Phys. Chem. A*, **116**, 1956 (2012); https://doi.org/10.1021/jp211382u
3. R.E. Vizhi, R.A. Kumar, D.R. Babu, K. Sathiyanarayanan and G. Bhagavannarayana, *Ferroelectrics*, **413**, 291 (2011); https://doi.org/10.1080/00150193.2011.531194
4. J. Baran and A.M. Petrosyan, *Ferroelectrics*, **432**, 117 (2012); https://doi.org/10.1080/00150193.2012.707879
5. R. Notario, M.V. Roux, A.F.L.O.M. Santos and M.D.M.C. Ribeiro da Silva, *J. Chem. Thermodyn.*, **73**, 57 (2014); https://doi.org/10.1016/j.jct.2013.08.026
6. V.J. Thanigaiarasu, N. Kanagathara, K. Senthilkumar, G. Anbalagan and M.K. Marchewka, *J. Optoelectron. Adv. Mater.*, **22**, 393 (2020).
7. V.J. Thanigaiarasu, N. Kanagathara, R. Usha, V. Sabari and V. Natarajan, *Asian J. Chem.*, **33**, 203 (2020); https://doi.org/10.14233/ajchem.2021.22983
8. M.J. Frisch, G.W. Trucks, H.B. Schlegel, G.E. Scuseria, M.A. Robb, J.R. Cheeseman, G. Scalmani, V. Barone, B. Mennucci, G.A. Petersson, H. Nakatsuji, M. Caricato, X. Li, H.P. Hratchian, A.F. Izmaylov, J. Bloino, G. Zheng, J.L. Sonnenberg, M. Hada, M. Ehara, K. Toyota, R. Fukuda, J. Hasegawa, M. Ishida, T. Nakajima, Y. Honda, O. Kitao, H. Nakai, T. Vreven, J.A. Montgomery Jr., J.E. Peralta, F. Ogliaro, M. Bearpark, J.J. Heyd, E. Brothers, K.N. Kudin, V.N. Staroverov, R. Kobayashi, J. Normand, K. Raghavachari, A. Rendell, J.C. Burant, S.S. Iyengar, J. Tomasi, M. Cossi, N. Rega, J.M. Millam, M. Klene, J.E. Knox, J.B. Cross, V. Bakken, C. Adamo, J. Jaramillo, R. Gomperts, R.E. Stratmann, O. Yazyev, A.J. Austin, R. Cammi, C. Pomelli, J.W. Ochterski, R.L. Martin, K. Morokuma, V.G. Zakrzewski, G.A. Voth, P. Salvador, J.J. Dannenberg, S. Dapprich, A.D. Daniels, O. Farkas, J.B. Foresman, J.V. Ortiz, J. Cioslowski and D.J. Fox, Gaussian 09 Citation, Gaussian, Inc., Wallingford CT (2009).
9. F. Weinhold and E.D. Glendening, NBO Version 3.1, TCI, Madison: University of Wisconsin (1998).
10. J.B. Foresman and A. Frisch, Exploring Chemistry with Electronic Structure Methods, Gaussian Inc. Pittsburgh (1996).
11. E.D. Glenening, A.E. Reed, J.E. Carpenter, F. Weinhold, J.A. Bohmann and C.M. Morales, NBO version 5.0, Theoretical Chemistry Institute University of Wisconsin Madison (2001).
12. T.K. Kuruvilla, J.C. Prasana, S. Muthu and J. George, *J. Mol. Struct.*, **1157**, 519 (2018); https://doi.org/10.1016/j.molstruc.2018.01.001
13. M. Khalid, A. Ali, M. Adeel, Z.U. Din, M.N. Tahir, E. Rodrigues-Filho, J. Iqbal and M.U. Khan, *J. Mol. Struct.*, **1206**, 127755 (2020); https://doi.org/10.1016/j.molstruc.2020.127755
14. S. Tariq, M. Khalid, A.R. Raza, S.L. Rubab, S.F.A. Morais, M.U. Khan, M.N. Tahir and A.A.C. Braga, *J. Mol. Struct.*, **1207**, 127803 (2020); https://doi.org/10.1016/j.molstruc.2020.127803
15. R. Zhang, B. Du, G. Sun and Y.X. Sun, *Biomol. Spectrosc.*, **75**, 1115 (2010); https://doi.org/10.1016/j.saa.2009.12.067
16. K. Fukui, Theory of Orientation and Stereoselection, Reactivity and Structure, Concepts in Organic Chemistry, Springer: Berlin (1975).
17. R.G. Parr, L.V. Szentpály and S. Liu, *J. Am. Chem. Soc.*, **121**, 1922 (1999); https://doi.org/10.1021/ja983494x
18. M.V. Putz, *The Scientific World J.*, **2013**, 348415 (2013); https://doi.org/10.1155/2013/348415
19. P.K. Chattaraj, U. Sarkar and D.R. Roy, *Chem. Rev.*, **106**, 2065 (2006); https://doi.org/10.1021/cr040109f
20. P. Politzer and D.G. Truhlar, Chemical Applications of Atomic and Molecular Electrostatic Potentials; Plenum: New York, NY, USA (1981).
21. J.S. Murray and K. Sen, Molecular Electrostatic Potentials: Concepts and Applications; Elsevier: Amsterdam, The Netherlands (1996).
22. E. Scrocco and J. Tomasi, Eds.: P.O. Lowdin, Electronic Molecular Structure, Reactivity and Intermolecular Forces: An Heuristic Interpretation by Means of Electrostatic Molecular Potentials, In: Advances in Quantum Chemistry, Academic Press, New York, p. 115 (1978).
23. N. Kanagathara, R. Usha, V. Natarajan and M.K. Marchewka, *Inorg. Nano Met Chem*., (2021); https://doi.org/10.1080/24701556.2021.1891103
24. S. Muthu and S. Renuga, *Biomol. Spectrosc.*, **132**, 313 (2014); https://doi.org/10.1016/j.saa.2014.05.009
25. S. Gunasekaran, S. Kumaresan, R. Arunbalaji, G. Anand, S. Seshadri and S. Muthu, *J. Raman Spectrosc.*, **40**, 1675 (2009); https://doi.org/10.1002/jrs.2318
26. M. Turner, J. McKinnon, S. Wolff, D. Grimwood, P. Spackman, D. Jayatilaka and M. Spackman, Crystal Explorer17, University of Western Australia Crawley, Western Australia, 541 Australia (2017).
27. M.A. Spackman and D. Jayatilaka, *CrystEngComm*, **11**, 19 (2009); https://doi.org/10.1039/B818330A